

VARIATION OF TEMPERATURE FIELD CREATED AT PULSED LASER IRRADIATION OF AMORPHOUS $\text{Fe}_{73.7}\text{Si}_{15.5}\text{B}_{7.4}\text{Nb}_{2.4}\text{Cu}_{1.0}$ ALLOY

YULIA S. NYKYRUY AND STEPAN I. MUDRY

*Ivan Franko Lviv National University, Physics of Metals Department
Kyrylo and Mephodiy Str. 8, 79005 Lviv, Ukraine*

(received: 9 December 2014; revised: 14 January 2015;
accepted: 21 January 2015; published online: 20 February 2015)

Abstract: The temperature in the laser irradiation area of an amorphous iron-based ribbon was calculated. As a result of the calculation a spatial temperature distribution and its time dependence were structured which allowed reproducing the geometric and structural characteristics of exposed areas. Simultaneously, an irradiated amorphous alloy was investigated by scanning electron microscopy which allowed determining the geometric and structural characteristics of these areas experimentally and obtaining their dependencies on the laser pulse parameters. The results of theoretical calculations were compared with the experimental data.

Keywords: laser irradiation, temperature distribution, amorphous materials, numerical method of finite differences

1. Introduction

Amorphous metal alloys due to their unique properties have been the subject of thorough experimental studies for a long time. In recent years, the intensity of these investigations has increased especially due to the possibility of forming nanocrystalline materials. Heating of an amorphous material leads to the transition from the metastable state to the equilibrium one, resulting in the formation of crystalline phases, the grain size, structural arrangement and chemical composition of which depend on the heating conditions, including the heating-cooling rate and the temperature. Laser irradiation, which is one of the tools for modification of the structure of amorphous alloys, leads to non-equilibrium heating and cooling of the material and a non-uniform temperature distribution. In view of this there is a relevant problem of determining the local conditions of nucleation that depend on the parameters of exposure.

The main and most currently approved models of interaction of laser radiation with the materials are described in [1–3]. According to them, laser radiation, which is directed to the surface of the material, partly reflects and partly absorbs. The reflected wave forms in the surface layer (skin – layer), whose thickness in metals for infrared optical range is $< 1 \mu\text{m}$. The intensity of the reflection is determined by the reflection coefficient (A), which depends on the material type and radiation wavelength.

Analytical equations for thermal processes under different conditions of laser material processing are presented in [4, 5]. However, according to [5], the results of calculations according to formulas do not always agree with experimental data, which restricts their application. This is because the thermal parameters are not constant during an actual laser heating process. For more accurate calculation the dependence of thermo-physical properties of the material at the rapid heating and cooling should be taken into account. Thus, in order to obtain correct results, it is necessary to solve nonlinear differential equations of heat conduction. The problem is further complicated by the nonlinearity of the boundary conditions, and by the absorption capacity temperature dependence. Thus, the heat equation for the problem of laser treatment is a system of nonlinear differential equations and general solution methods considering these nonlinearities in the theory of heat conduction are missing. Therefore, approximate methods and solutions based on analytical representations, numerical methods, etc. are commonly used. One of them was used in this work to study the evolution of the temperature field under the influence of laser irradiation. It was particularly the numerical method that was used, with accounting for the linear approximations of the temperature dependence of the coefficients of specific heat, thermal conductivity and thermal diffusivity.

2. Experimental

The amorphous alloy $\text{Fe}_{73.7}\text{Si}_{15.5}\text{B}_{7.4}\text{Nb}_{2.4}\text{Cu}_{1.0}$ was obtained by melt spinning in the form of ribbons 1–2 cm wide and approximately $25 \mu\text{m}$ thick. Irradiation was carried out in air atmosphere using pulsed laser radiation at the scanning modes of exposure, with the parameters presented in Table 1. The samples were fastened on a flat table and the laser beam was focused on the sample surface in a spot with diameter d_{ef} . The mode of radiation was a single-mode TEM_{00} , with the Gaussian distribution of intensity in the beam. The surface structure of amorphous ribbons in areas of laser irradiation was investigated by scanning electron microscopy.

3. Temperature distribution calculation method

Light absorption in metals occurs due to interaction of the electromagnetic wave with electrons. The excited electrons interacting with lattice phonons and other electrons, loss the energy that provides heat transfer. The average time between collisions of electrons in a conductor is of the order 10^{-13} s. As the value

Table 1. Radiation parameters

Wavelength λ , μm	1.06
Pulse duration τ , ns	130
Pulse energy E , mJ	0.1–0.4
Pulses frequency f , kHz	50
Effective diameter of the focal spot d_{ef} , μm	30

of the duration of the laser pulse used in the experiment is much more (10^{-7} s), the classical theory of heat conduction is applicable to calculate the time dependence of the temperature field [6]. The numerical method of finite differences was used to solve the problem. At the first stage of this procedure we used the method of building a 3-dimensional uniform grid with the cell size $\delta = 1 \mu\text{m}$ and the heat transfer between these cells occurred through imagined walls. In a non-stationary process the heat passes in and out in each cell changing its internal energy. In the calculation of the irradiated area temperature the Gaussian distribution of radiation intensity allowed us to determine the “radiation dose” E^{xy} , for each irradiated cell with x, y coordinates (Figure 1). The method, which is based on the splitting of three-dimensional equation into a simpler – one-dimensional equation along each axis (X, Y, Z) (coordinate-wise splitting method [7, 8]) was used to solve the problem of heat distribution. The heat transfer from a cell to any neighbor cells occurs under the Fourier law, which for the one-dimensional case is $q = -k(dT/dx)$. Applying the method of finite differences, we obtain the energy by heat transfer:

$$E_h = q\Delta S = -(k/\delta)\Delta T\Delta tS \quad (1)$$

where ΔT – the temperature difference between adjacent cells, and S – the surface area through which the heat flows, which for the one-dimensional case is $S = \delta \times \delta$. The change in internal energy (input and output heat difference) of the considered cell during Δt is:

$$E'_n = c_p\rho V\Delta T' = c_p\rho V(T' - T) \quad (2)$$

where T – the temperature in the cell at current time t , T' – the temperature in the cell at time $t + \Delta t$; c_p and ρ – the specific heat coefficient and density, respectively. In applying the numerical method of finite differences the formula for calculation is reduced to a form where the forthcoming temperature of the cell is a function of time and of the current temperature of this cell and of current temperatures of adjacent cells. Such equations need to be designed for all cells of the area under investigation.

The method of thermal balance was also used in the calculation procedure. The interrelation between the major heat sources and heat dissipation can be described by the following balance equations:

$$E - (A \times E + E_h + E_{\text{melt}} + E_{\text{ev}}) = E'_n \quad (3)$$

where E – the laser pulse energy; A – the refraction coefficient; E_h – energy losses caused by heat transferring, E_{melt} , and E_{ev} – specific heat of melting and

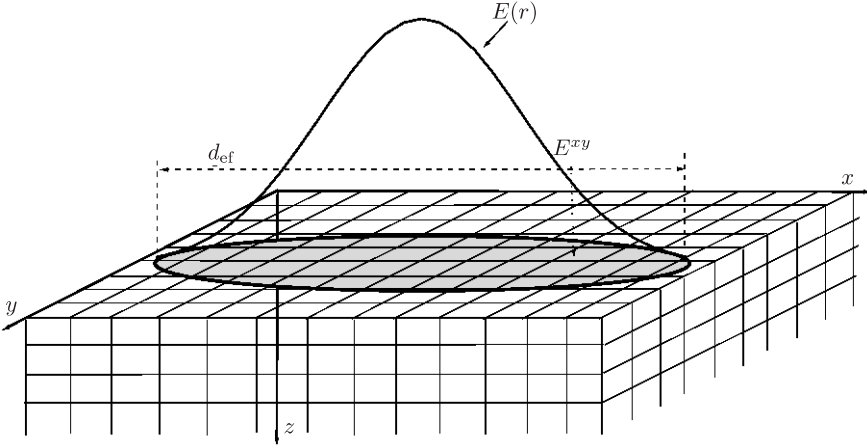


Figure 1. Interpretation of radiation zone

evaporation of the material, respectively, E'_n – the internal energy of the cell. When the radiation flow is over, any further temperature distribution is mainly determined by the heat transfer process.

The time dependence of temperature as well as the spatial temperature distribution were simulated. An average linearly interpolated temperature dependence of heat capacity c_p) and heat conductance coefficients (k), obtained from experimental data for Fe-based amorphous alloys [9–11] were used. These values were obtained to be:

$$\begin{aligned} c_p &= 401 + 0.51 \times T, \text{ subject to } T_{\text{room}} < T < T_{\text{melt}} \\ c_p &= 938 \text{ J/kg}\cdot\text{K}, \text{ subject to } T > T_{\text{melt}} \end{aligned} \quad (4)$$

$$\begin{aligned} k &= 3 + 0.021 \times T, \text{ subject to } T_{\text{room}} < T < T_{\text{melt}} \\ k &= 40 \text{ W/m}\cdot\text{K}, \text{ subject to } T > T_{\text{melt}} \end{aligned} \quad (5)$$

Parameters A , ρ , E_{melt} and E_{ev} correspond to those for crystalline iron [12].

4. Results and discussions

The temperature variation during pulse laser irradiation was analyzed for different energies. For instance the results of calculation for the energy values $E = 0.114$ (a), 0.134 (b), 0.197 (c) and 0.245 mJ (d) (Figure 2) show that at pulse energy value $E = 0.114$ mJ the temperature of the focused spot enter rises up to the iron melting temperature, so the melting of surface layers can be predicted. Thus, the local melting results in changes in the surface topology and this can be confirmed by a microscopic analysis. As follows from our results the melting process cannot be reached at lower energy. At higher energy values ($E = 0.197$ mJ) the temperature rises up to the boiling temperature of iron (Figure 2.c), so the intensive evaporation of surface layers is predicted to occur. Such local evaporation results in forming craters, which can be indicated by microscopic analysis too.

The obtained results allow evaluating the melting zone radius which can be determined from the maximum profile analysis, as is shown in Figure 3. For

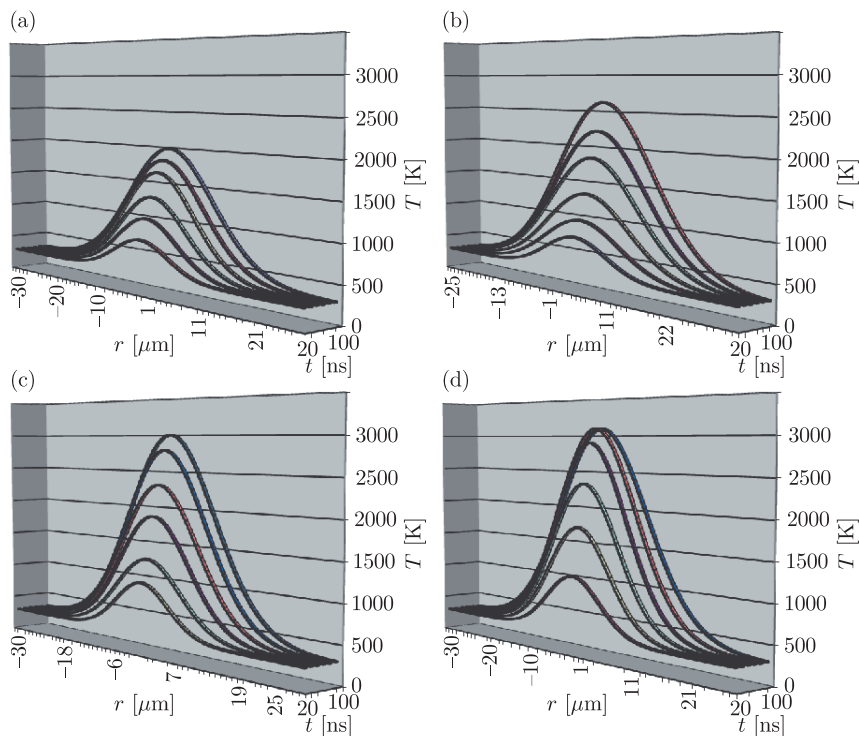


Figure 2. Local temperature variation during pulse action: $E = 0.114$ (a), 0.134 (b), 0.197 (c), 0.245 mJ (d)

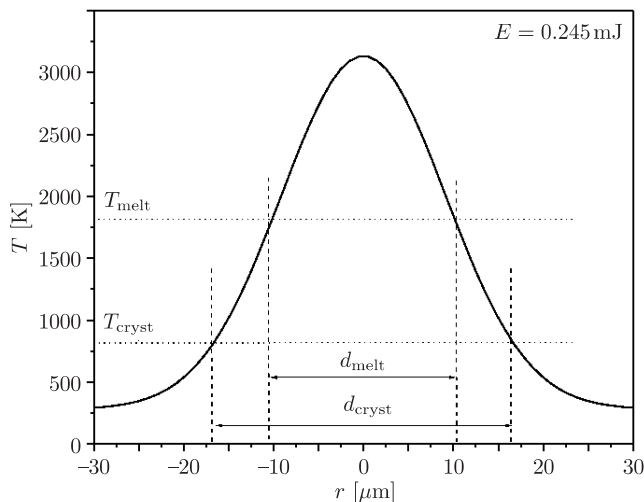


Figure 3. Temperature distribution at the end of pulse action ($E = 0.245$ mJ)

example, the melting zone radius for $E = 0.245$ mJ is found to be $r_{\text{melt}} \approx 11 \mu\text{m}$. As a result of this procedure the energy dependence of the radius was determined. At the same time this method allows evaluating the size and form of the zone

with conditions ($T_{\text{cryst}} \leq T \leq T_{\text{melt}}$) favorable for crystallization. The size of such a zone is restricted by r_{cryst} and r_{melt} and it is circle-like at low values of energy (< 0.11 mJ), while at higher values it transforms to being ring-like. The parameter T_{cryst} was assumed to be as an average temperature of crystallization for the Fe-Nb-Cu-Si-B alloy ($T_{\text{cryst}} = 800$ K)

The time dependencies of temperature for center and boundary points of the focal spot at the indicated energy values (Figure 4) allowed us to evaluate the cooling rates, which were found to be $\sim 10^9$ K/s at the start of cooling and decreased to about 10^7 K/s when the temperature was reduced to T_{cryst} . The obtained values are much higher than the critical cooling rate at the spinning process (10^6 K/s).

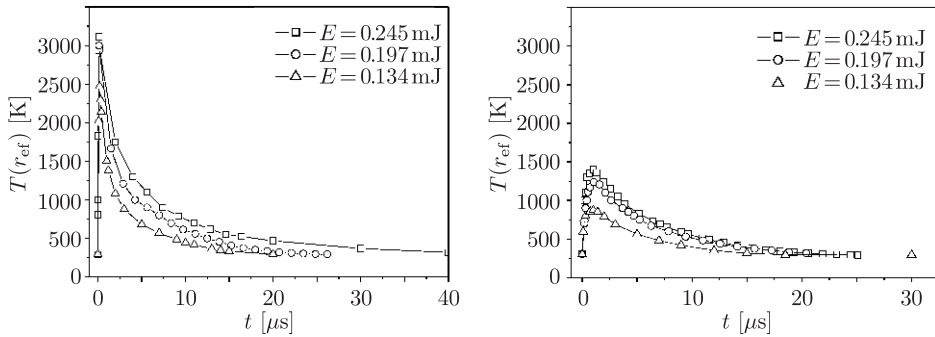


Figure 4. Time dependence of temperature at central (a) and boundary (b) points of focal spot

The irradiated surface of the ribbon was investigated by raster electron microscopy. The results of the microscopic analysis confirm the existence of melting zones and craters predicted by calculation. The structure of surface irradiated at $E = 0.114$, 0.134 , and 0.168 mJ is shown in Figure 5.

The results, obtained by microscopic analysis, show that changes in surface topology begin to occur when $E \geq 0.114$ mJ whereas at $E \geq 0.168$ mJ the irradiated surface reveals craters. We suppose that these changes are related to local surface melting and evaporation processes, respectively. Using software we estimated the average radiuses of melting zones as well as the radius dependence on energy (Figure 6).

The comparison of results of experimental investigation of microstructure of the irradiated surface with the calculated data shows a good agreement. The predicted pulse energy values that correspond to the melting are in accordance with the experimental data. It follows from the calculations that the cooling rates are higher than the critical value at melt spinning. As far as cooling occurs while the liquid phase exist, reamorphization is expected to occur as a result. The results of the X-ray diffraction show an amorphous structure of irradiated samples [13]. The radius values of the melt zones, evaluated by calculation coincide with the experimentally evaluated ones with accuracy of less than 10%.

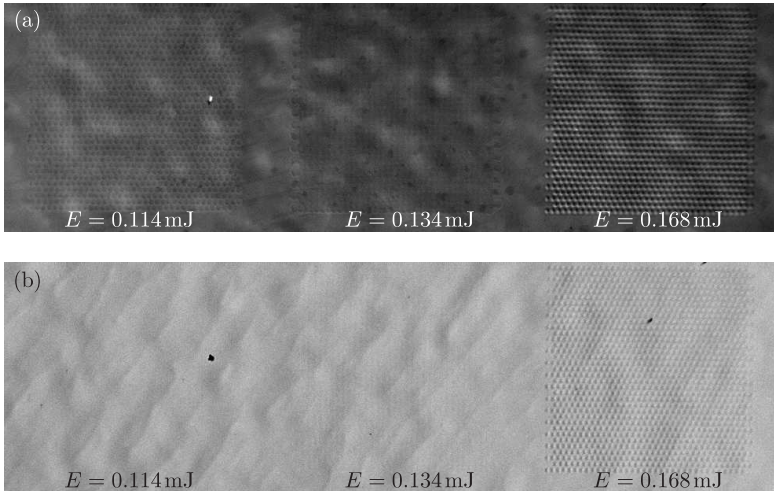


Figure 5. Irradiated surface: secondary electron analysis (a) backscattered electron analysis (b)

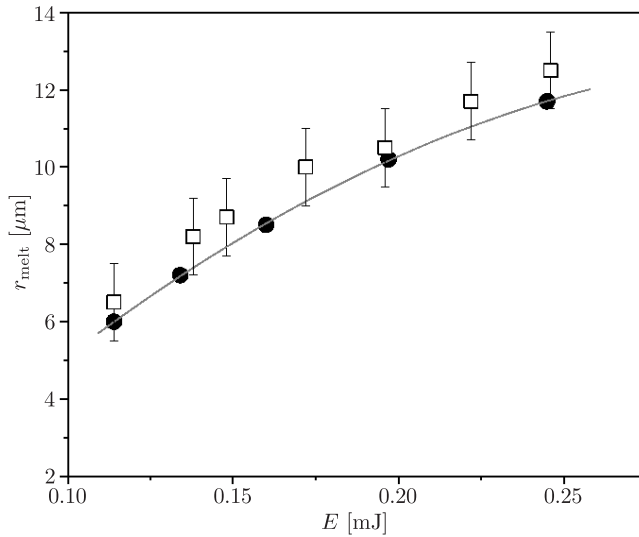


Figure 6. Radius dependence on energy; \square – experimental, \bullet – calculated

5. Conclusions

The applied calculation methods (the numerical method of finite differences, the coordinate-wise splitting method, the method of building a 3-dimensional uniform grid and thermal balance) well describe the actual processes of heating-cooling in an amorphous alloy under laser irradiation. Approximations, such as average linearly interpolated temperature dependencies of heat capacity and heat conductance coefficients as well as the parameters A , ρ , E_{melt} and E_{ev} corresponding to those for crystalline iron, provide a satisfactory precision of calculations of the spatial temperature distribution and its time dependence.

References

- [1] Steen W M 1991 *Laser Material Processing*, Springer-Verlag 266
- [2] 2001 *LIA Handbook of Laser Materials Processing* [editor in chief John F. Ready, associate editor Dave F. Farson], Magnolia Publishing 715
- [3] Ramanatey-Asiby Elijah, Jr. 2009 *Principles of laser material processing*, John Wiley & Sons, Inc. 820
- [4] Grigoryants A G 1994 *Basics of laser material processing*, (CRC Press, Inc 2000), MIR Publishers
- [5] Grigoryants A G, Shyganov I N, Misurov A I 2008 *Tehnologicheskie procesy lazernoj obrabotki: uchebnoe posobie (Technological processes of laser treatment: Manual)*, (in Russian), Bauman MSTU 664
- [6] Ready John F 1971 *Effects of high-power laser radiation*, Academic Press 468
- [7] Lukyanenko S O 2013 *Eastern-European Journal of enterprise technologies*, (in Russian) **6/5** (66) 12
- [8] Berezin S B, Paskonov V M, Sakharnykh N A 2012 *Alternating direction implicit numerical method for 3D fluid flow simulation using GPU*, *Vychislitel'nye Metody i Programirovanie*, (in Russian) **13** 75
- [9] Choy C L, Tong K W, Wong H K, Leung W P 1991 *Thermal conductivity of amorphous alloys above room temperature*, *J. Appl. Phys.* **70** 4919
- [10] Jezowski A, Mucha J, Pompe G 1987 *Thermal conductivity of the amorphous alloy $Fe_{40}Ni_{40}P_{14}B_6$ between 80 and 300 K*, *J. Phys. D: Appl. Phys.* **20** 1500
- [11] Suzuki K, Cadogan J M, Aoki K, Tsai A P, Inoue A, Masumoto T 2001 *Nanocrystallization and glass transition in Cu-free Fe-Nb-B soft magnetic alloys*, *Scripta mater.* **44** 1417
- [12] 1965 *Fiziko-khimicheskie svoistva elementov: Spravochnik (Physicochemical Properties of Elements: A Handbook)* Samsonov G V (ed.), Naukova Dumka
- [13] Mudry S I, Scherba I D, Nykyruy Y S 2014 *Laser induced structure transformation in Fe-Cu-Nb-Si-B amorphous alloy*, *Annales Akademie Paedagogicae Cracoviensis / Studia Technica VII* 42